Homoepitaxial Growth of Iron and a Real Space View of Reflection-High-Energy-Electron Diffraction

Joseph A. Stroscio, D. T. Pierce, and R. A. Dragoset

Electron Physics Group, National Institute of Standards and Technology, Gaithersburg, Maryland 20899

We report real space views of the homoepitaxial growth of Fe on Fe(001) whiskers observed by scanning tunneling microscopy. A measure of the surface diffusion of the Fe atoms is obtained over the temperature range of 20–250 °C. The effect of the diffusion kinetics is observed in the surface morphology as a decrease in the interface width with temperature. Measurements of reflection-high-energy-electron diffraction during growth allow a comparison of real and reciprocal space techniques.

Molecular beam epitaxy (MBE) is a method of materials growth used to produce artificial structures with abrupt interfaces at the single atomic layer level. The process consists of forming an atomic or molecular beam which impinges on a surface held at some temperature. The nonequilibrium nature of MBE, in most applications, leads to a supersaturation of adsorbed species, which must undergo complicated processes such as, dissociation, diffusion, nucleation, and film growth. The most widely used technique to study MBE growth has been reflection-high-energy-electron diffraction (RHEED) [1], in which a high energy (typically $\sim$10–30 keV) electron beam strikes a surface at grazing incidence and the resulting diffraction pattern is monitored. Early measurements of RHEED during growth showed the astonishing feature that the intensity of the diffraction features oscillates in time [2]. Through detailed modeling of RHEED oscillations, there have been attempts to extract information on the surface morphology and processes such as diffusion and nucleation, but real space measurements of these processes have been lacking [1]. Central to interpreting RHEED oscillations is knowing how kinetic effects such as diffusion and nucleation influence RHEED oscillations. What do RHEED oscillations indicate about surface roughness and morphology? When do RHEED oscillations imply layer-by-layer growth? Even the simple question, "What is oscillating in the growth process that gives rise to the RHEED oscillations?", has not been fully answered [1,3–5].

We report on measurements of the homoepitaxy of Fe to gain an understanding of the growth processes and how these affect RHEED measurements. Iron homoepitaxy was chosen as it avoids the complications of dissociation and multiple component systems. The diffusion of Fe on the Fe(001) surface is measured over the range of temperatures from 20 to 250 °C, and yields an activation energy barrier for surface diffusion of 0.45 ± 0.08 eV. The effect of diffusion is observed in RHEED intensity oscillations as well as in surface morphology measured with scanning tunneling microscopy (STM) on the same samples. These measurements constitute some of the first real space views of the growth morphology that is associated with particular RHEED intensity oscillation behav-

ior and give insight into the growth process.

The experiments were performed in an ultra-high-vacuum system, with both STM and RHEED capabilities, which is described elsewhere [6]. RHEED measurements were made using a 10 keV electron beam and digitally recording the diffraction patterns in real time. STM measurements were made at the same sample location as the RHEED measurements to within ±0.5 mm. The Fe(001) whiskers used for the substrates had approximately one single-atom-high step per μm. Previous RHEED measurements have shown this crystal quality yields nearly perfect RHEED patterns from these surfaces [7].

A measure of the diffusion of Fe atoms on Fe surfaces can be obtained from examining the temperature dependence of the density of Fe islands produced for a fixed *low* surface coverage, as shown in Fig. 1. In examining Figs. 1(a)–1(c), nucleation and growth of islands are seen to be competing processes; as the diffusion length of the Fe atoms increases, the probability of incorporation into an existing island (growth) increases over nucleation. In Fig. 1(d), the island density shows an Arrhenius dependence on temperature for $T < 250$ °C, due to the activated process of diffusion. Above 250 °C, a large decrease in island density is observed due to the additional process of coarsening. Below 250 °C, the island densities can be analyzed using a rate equation analysis [8–10] to yield the tracer diffusion coefficient D of single Fe atoms on the Fe(001) surface, shown by the solid symbols in Fig. 1(d) [11]. Fitting the diffusion data to an Arrhenius form, $D = D_0 e^{-E/kT}$, yields an activation energy $E = 0.45 \pm 0.08$ eV, and a prefactor $D_0 = 7.2 \times 10^{-4}$ cm^{2}s^{-1}.

The surface diffusion coefficient varies greatly over the 20–250 °C temperature range. When comparing the diffusion coefficient with an incident flux of $\sim$1 monolayer (ML)/min (2×10^{13} atoms cm^{-2}s^{-1}), the competition between nucleation and growth is expected to lead to a kinetically limited roughening of a growing Fe film at the lower temperatures [12]. The effect of the diffusion kinetics on the growth of thin films is directly observed in Fig. 2, which shows RHEED intensity measurements of the (0,0) diffracted beam during growth and the STM images of the surface morphology after growth was
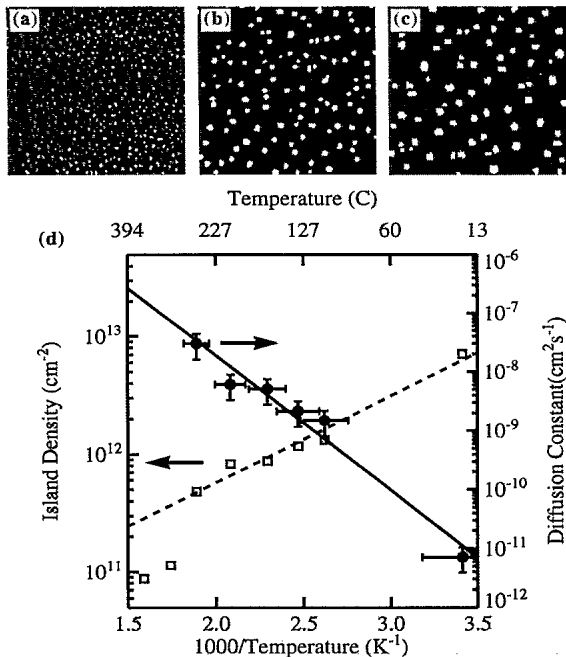
FIG. 1. (a)–(c) STM images, 100×100 nm, of single layer Fe islands (white) on the Fe(001) surface (black). Sample temperatures during growth are (a) 20°C, (b) 108°C, and (c) 163°C. (d) The temperature dependence of the density of Fe islands (open squares) obtained from STM measurements as in (a)–(c), and the deduced diffusion constant (solid circles) from a rate equation analysis of the island density [11]. The lines are least-square fits to the data for $T \leq 250\,°C$. The error bars indicate the variation in incident flux and uncertainties in the temperature measurement. Fe was deposited for a fixed time for all measurements with a flux of $(1.4 \pm 0.3) \times 10^{13}$ atoms $cm^{-2}s^{-1}$, yielding a coverage of 0.07 ± 0.016 ML (1 ML $= 1.214 \times 10^{15}$ atoms cm^{-2}).
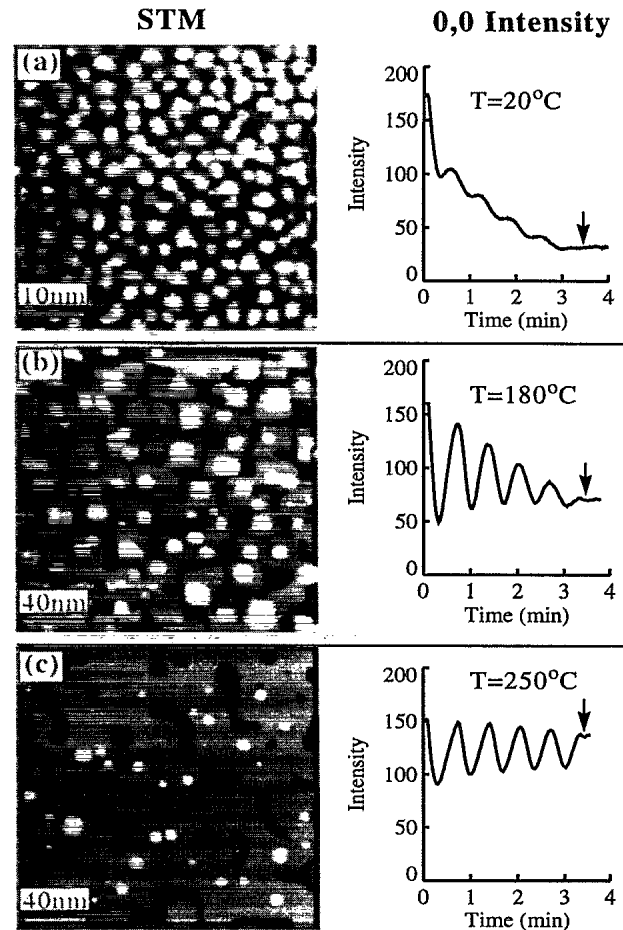

FIG. 2. STM and RHEED (0,0) beam intensity measurements of Fe on Fe(001) growth obtained on the same samples. All the films were grown for five RHEED oscillations, at which time the Fe flux was turned off, indicated by the arrows in the RHEED plots. The RHEED measurements were made with a 10 keV beam at the antiphase angle of incidence of 64 mrad. The intensity plots were obtained by integrating over the (0,0) diffraction spot by $\pm 0.05°$ in both directions. Sample temperatures during growth, rms roughness, and step densities are (a) 20°C, 0.116 nm, 1.74 nm^{-1}; (b) 180°C, 0.095 nm, 0.23 nm^{-1}; and (c) 250°C, 0.06 nm, 0.09 nm^{-1}. STM images are shown in a grey scale with black being the lowest height level. The major changes in grey level indicate a monatomic step. Image sizes are (a) 50×50 nm and (b), (c) 200×200 nm.

stopped at five oscillations. The surface morphology for growth at 20°C, shown in Fig. 2(a), consists of a terraced structure with five layers exposed and a rms roughness of 0.116 nm. The predominant island structure has a mean spacing of ~5 nm and gives rise to a splitting of the diffraction beams in the RHEED measurements, discussed below. The (0,0) RHEED beam intensity is observed to oscillate with time, but with a pronounced decay in intensity.

A much larger terrace structure is observed in Fig. 2(b) for growth at 180°C where the diffusion coefficient has increased by a factor of 600 compared to its value at 20°C [see Fig. 1(d)]. The RHEED intensity during growth shows stronger oscillations, but still decays and damps considerably by the fifth oscillation. Interestingly, there are still five layers exposed and the rms roughness is 0.095 nm, very close to the 20°C measurement. The decrease in the RHEED intensity envelope in Figs. 2(a) and 2(b) is consistent with kinematic analysis for the out-of-phase condition which predicts an exponential dependence on the surface roughness [13,14]. The larger terraces in the 180°C growth lead to a step density that is

almost an order of magnitude less than for growth at 20°C, 0.23 nm^{-1} compared to 1.74 nm^{-1}.

The growth observed at 250°C in Fig. 2(c) is nearing the layer-by-layer growth mode. There are only three layers exposed, with one layer clearly dominant, and the rms roughness is 0.06 nm. At this temperature the RHEED oscillations are only slightly damped, and the intensity returns to nearly its original value with each oscillation. This is the RHEED intensity oscillation signature of near perfect layer-by-layer growth.

Central to the interpretation of RHEED is understanding what is changing in the MBE growth process to give

TABLE I. Coverage, Θ, in monolayers, rms roughness (W), step densities (SD), exposed layer occupation, $\Theta_n - \Theta_{n+1}$, where Θ_n is the coverage of the nth layer in monolayers, and an estimate of the kinematic intensity at the antiphase condition, $I(S=0) = |\sum_n (-1)^n (\Theta_n - \Theta_{n+1})|^2$, for various Fe thicknesses and growth at 250 °C corresponding to the STM images shown in Figs. 2 and 3. The step density is defined as the step edge length per unit area.

| | RHEED oscillations | | | |
	3.5	4.0	4.5	5.0
Θ	3.32	3.97	4.27	4.85
W (nm)	0.075	0.069	0.084	0.062
SD (nm^{-1})	0.13	0.12	0.17	0.09
100I	7.4	27.7	4.8	33.9
$\Theta_6 - \Theta_7$	0.0	0.0	0.005	0.030
$\Theta_5 - \Theta_6$	0.002	0.104	0.325	0.791
$\Theta_4 - \Theta_5$	0.340	0.763	0.604	0.179
$\Theta_3 - \Theta_4$	0.634	0.133	0.066	0.0
$\Theta_2 - \Theta_3$	0.024	0.0	0.0	0.0

rise to the observed RHEED intensity oscillations. There have been two schools of thought that have explained the origin of RHEED oscillations. In one case the oscillations have been understood in terms of a kinematic interference effect, where the oscillations result from destructive interference between consecutive surface layers at the antiphase diffraction geometry [5,13]. The alternate explanation is that the intensity oscillations are not due to an interference effect, but result from diffuse scattering from step edges [3,4]. To try to determine which explanation is correct, we compare the surface morphology of a film grown for an integer number of oscillations to that grown for a half-integer number of oscillations. Figures 3(a)–3(c) and Fig. 2(c) show the surface morphology for films grown for 3.5, 4, 4.5, and 5 RHEED oscillations at $250 \pm 20\,°C$. The coverage, step density, surface roughness, and layer occupations determined from the STM images are listed in Table I. The coverages determined from the STM measurement are seen to correspond to the number of RHEED oscillations to within (10–20)% of a monolayer. Some of this

FIG. 3. (a)–(c) STM images after growing Fe on Fe(001) at a sample temperature $250 \pm 20\,°C$ for various numbers of RHEED oscillations: (a) 3.5, (b) 4.0, and (c) 4.5 oscillations. The corresponding coverages determined from the STM images are 3.32, 3.97, and 4.27 monolayers, respectively. Image sizes are all 200×200 nm.

discrepancy may be due simply to the timing of the closing of the shutter in the evaporation and/or surface inhomogeneities due to a nonuniform flux.

As seen in the images in Fig. 3 and in Table I, the growth oscillates from a rougher, partially filled surface with nearly a half-filled layer exposed to a smoother surface with nearly a complete layer filled. This is the growth expected from a nucleation and growth mode. In any growth model which oscillates between a rough and smooth surface, the step density will also oscillate, as observed in Table I. The calculated kinematic intensity resulting from the destructive interference between the surface layers, shown in Table I, is observed to oscillate strongly. Since both quantities are oscillating, a clear distinction between the kinematic versus step edge scattering models is not possible. More likely, both mechanisms contribute to the intensity oscillations, and their relative importance depends on the particular diffraction conditions. We note, however, that the 180 °C growth [Fig. 2(b)] showed a strong decay in RHEED intensity oscillations, similar to the 20 °C growth [Fig. 2(a)], although the step density decreased nearly an order of
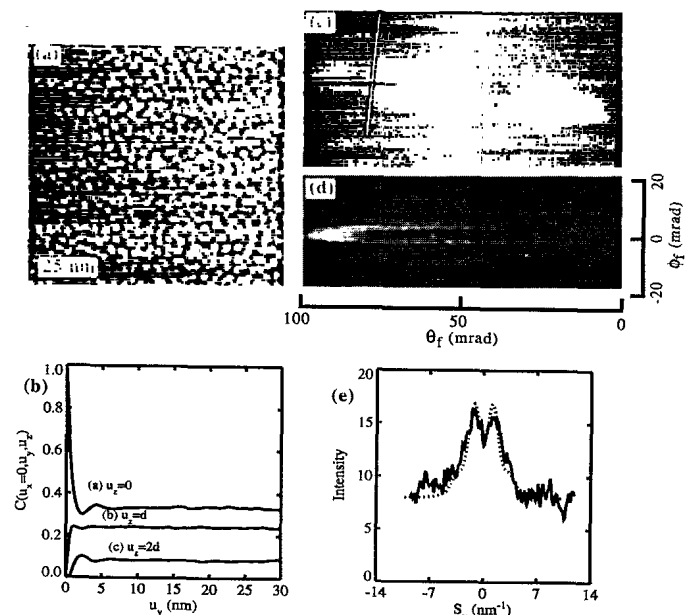
FIG. 4. (a) STM image, 100×100 nm, of Fe grown at 20 °C for a thickness corresponding to three RHEED oscillations. (b) Pair correlation function obtained from the STM image in (a), plotted for separations in the vertical direction u_y, and step height difference $u_z = 0$, $1d$, and $2d$, where $d = 0.144$ nm. (c) RHEED (0,0) diffraction streak observed after growing Fe on Fe(001) for three RHEED oscillations. The initial RHEED pattern before growth was a single spot at $\theta_f = 64$ mrad. (d) The calculated diffuse scattering using Eq. (1) for the RHEED geometry. The angular scale is the same for (c) and (d). (e) A comparison of measured and calculated RHEED intensities vs momentum transfer along the y directions, ϕ_f, indicated by the line in (c) at $\theta_f = 80$ mrad. Solid line, measured profile from (c); dotted line, calculated profile from (d).

magnitude, pointing to the importance of surface roughness in the RHEED intensity oscillations in the antiphase diffraction geometry.

Within the kinematic model, the Bragg scattering and the diffuse or non-Bragg scattering due to the presence of steps can be calculated exactly using the measured surface topography [15,16]. Such a calculation provides an illustration of the kinematic diffraction theory and also shows how the surface roughness in the room temperature growth appears in RHEED measurements. As mentioned above, the growth of Fe at room temperature gives rise to a splitting of the RHEED diffraction beams, which develops during the first RHEED intensity oscillation. The splitting of the (0,0) beam measured after three RHEED oscillations is shown in Fig. 4(c). The corresponding surface is shown in Fig. 4(a). In the kinematic theory of RHEED, the intensity is given by the Fourier transform of the surface pair correlation function as

$$I(S) = N \sum_{u} e^{-i(S \cdot u)} C(u) , \qquad (1)$$

where N is the number of surface scatterers and S is the momentum transfer. $C(u)$ is the pair correlation function of the surface atoms and is the probability of finding two scatterers on the surface separated by the three-dimensional vector u. Figure 4(b) shows the pair correlation function calculated from the image in Fig. 4(a) and displayed for displacements u_y along the vertical direction in Fig. 4(a) (the same direction in which the splitting is observed) for three different height differences u_z (u is broken down into surface parallel and perpendicular parts, where u_z denotes surface atoms separated by layer height differences nd, d being the interlayer spacing). The peak at $u_y \cong 5$ nm in the $u_z = 0$ correlation corresponds to the average distance between the center of one island and the next. Figure 4(d) shows the calculated diffuse intensity pattern for the RHEED geometry using Eq. (1). The diffuse intensity, which is due to the lack of long-range order due to the presence of steps, is calculated by subtracting off the nonvarying constant term from the pair correlation function; the constant term gives rise to the Bragg contribution to the scattering and is small compared to the non-Bragg contribution in Fig. 4(d) [15,16]. The (0,0) beam exhibits a very similar splitting in the ϕ_f direction to that observed experimentally. A comparison between the measured and calculated profile is shown in Fig. 4(e) along the line indicated in Fig. 4(c) at $\theta_f = 80$ mrad. The splitting of the (0,0) beam of 2.3 nm^{-1} corresponds to a real space period of 5.4 nm, which is the characteristic distance of the island structures in Fig. 4(a). While good agreement is obtained between the measured and calculated rod splitting, it is also seen that the kinematic approximation does not reproduce all the intensity variation seen along the (0,0) rod in the θ_f direction and that more complicated scattering events need to be included.

In summary, we have measured the diffusion of Fe

atoms on Fe(001) surfaces over the 20–250 °C temperature range by analyzing the Fe island densities observed in STM measurements. The effect of diffusion kinetics dominates the growth for the conditions studied here for Fe homoepitaxy. Simultaneous RHEED measurements and STM measurements on the same samples have given a real space view of the growth morphology associated with particular RHEED intensity oscillation behavior.

[1] See, for example, *Reflection High Energy Electron Diffraction and Reflection Electron Imaging of Surfaces*, edited by P. K. Larsen and P. J. Dobson, NATO ASI Ser. B, Vol. 188 (Plenum, New York, 1988).

[2] J. H. Neave, B. A. Joyce, P. J. Dobson, and N. Norton, Appl. Phys. A **31**, 1 (1983); J. M. Van Hove, C. S. Lent, P. R. Pukite, and P. I. Cohen, J. Vac. Sci. Technol. B **1**, 741 (1983).

[3] S. Clarke and D. D. Vvedensky, Phys. Rev. Lett. **58**, 2235 (1987); J. Appl. Phys. **63**, 2272 (1988).

[4] J. Sudijono, M. D. Johnson, C. W. Snyder, M. B. Elowitz, and B. G. Orr, Phys. Rev. Lett. **69**, 2811 (1992).

[5] G. S. Petrich, P. R. Pukite, A. M. Wowchak, G. J. Whaley, P. I. Cohen, and A. S. Arrott, J. Cryst. Growth **95**, 23 (1989).

[6] J. A. Stroscio, D. T. Pierce, R. A. Dragoset, and P. N. First, J. Vac. Sci. Technol. A **10**, 1981 (1992).

[7] A. S. Arrott, B. Heinrich, and S. T. Purcell, in *Kinetics of Ordering and Growth at Surfaces*, edited by M. G. Lagally (Plenum, New York, 1990), p. 321.

[8] J. A. Venables, Philos. Mag. **27**, 697 (1973).

[9] Y. W. Mo, J. Kleiner, M. B. Webb, and M. G. Lagally, Phys. Rev. Lett. **66**, 1998 (1991); Surf. Sci. **268**, 275 (1992).

[10] M. C. Bartelt and J. W. Evans, Phys. Rev. B **46**, 12675 (1992).

[11] Here we are assuming only single atoms are mobile on the surface (single atoms are not seen in the STM images), and are taking the island capture numbers to be unity. Previous analyses have shown that taking the capture numbers to be unity would not change the functional dependence on temperature (or the derived activation energy), but can affect the overall magnitudes of the diffusion coefficients through a multiplicative factor by less than a factor of 10 [8,9].

[12] Y.-L. He, H.-N. Yang, T.-M. Lu, and G.-C. Wang, Phys. Rev. Lett. **69**, 3770 (1992).

[13] P. I. Cohen, G. S. Petrich, P. R. Pukite, G. J. Whaley, and A. S. Arrott, Surf. Sci. **216**, 222 (1989).

[14] H. C. Kang and J. W. Evans, Surf. Sci. **271**, 321 (1992).

[15] C. S. Lent and P. I. Cohen, Surf. Sci. **139**, 121 (1984).

[16] A. K. Myers-Beaghton, Surf. Sci. **241**, 439 (1991).